Index Modulation Multiple-Access (IMMA): Efficient Techniques for Downlink Millimeter Waves Outdoor Channel

SAID EL-KHAMY (Life Fellow, IEEE), HASSAN M. ELRAGAL, AND REMON A. POLUS ⓘ (Student Member, IEEE)

Department of Electrical Engineering, Faculty of Engineering, Alexandria University, Alexandria 11432, Egypt

CORRESPONDING AUTHOR: REMON A. POLUS (e-mail: es-remon.adly1116@alexu.edu.eg).

ABSTRACT   In this paper, we propose two new multiple-access schemes for downlink transmission based on the combination of orthogonal frequency division multiplexing (OFDM) with index modulation (IM), namely OFDM-IM. In the first proposed technique, namely, Index Modulation Multiple-Access (IMMA), the OFDM subcarriers are divided into multiple sets, and each set is assigned to a specific user, and their data bits are transmitted via the OFDM-IM technique. On the other hand, in the second proposed scheme, an extended version of IMMA is introduced where the different users are arranged into different pairs, and each pair of users shares a block of OFDM subcarriers. The two users of each pair are allocated into different domains: the index domain and the constellation domain. The focus in this paper is on the 28 GHz transmission band as it has been considered for an initial deployment of mm-waves wireless systems due to their relatively lower location within the mm-waves range and are hence characterized by lower attenuation. The fluctuating two ray model (FTR) was proposed as the propagation model for 28 GHz outdoor millimeter waves channels. Simulation results demonstrate that both schemes achieve improved average bit error rate (ABER) than classical OFDMA and NOMA-IM techniques.

INDEX TERMS   5 G, Index modulation, millimeter waves, multiple-access, NOMA.

I. INTRODUCTION

Novel transmission techniques are being developed to meet the requirements of the fifth-generation (5 G) cellular network as the number of wirelessly connected devices grows in order to meet the vision of the Internet of Things (IoT) and Machine to Machine (M2M) communications, which is accompanied by spectrum scarcity and limited energy resources. It is predicted that the number of linked devices would rise 1000-fold [1]. Furthermore, improving spectral efficiency (SE) and energy efficiency (EE) are key goals for 5 G networks [2].

Non-orthogonal multiple access (NOMA) is recommended as the multiple-access approach for 5G [3], which seeks to serve many users over the same time-frequency resources to increase the number of connected users in order to satisfy these criteria. There are primarily two forms of NOMA: the first is power domain NOMA (PD-NOMA) [4], which assigns various power levels to different users using superposition

coding (SC) at the transmitter and successive interference cancellation (SIC) at the receiver. The second type is code domain NOMA, which assigns non-orthogonal spreading codes to various users. Low-density spreading (LDS) [5] and sparse code multiple access (SCMA) [6] are two examples of such codes. However, these NOMA techniques require complex detectors such as SIC and message passing algorithm (MPA) as in LDS and SCMA. Furthermore, inter-user interference (IUI) limits the performance of such NOMA schemes.

To avoid the restrictions of available bandwidth in the standard microwave band, new spectrum bands such as millimeter waves (mm-waves) have been researched for 5 G networks. The mm-waves band has traditionally covered a frequency range of 30 GHz to 300 GHz. The 28 GHz spectrum has attracted both research and academics for the early implementation of mm-wave communication systems. This is owing to the fact that they have a lower frequency in the mm-waves region, which results in less attenuation [7]. Fluctuating

two-ray (FTR) has recently been presented as a viable statistical channel model for the 28 GHz band, with better captures for the 28 GHz channel characteristics than traditional fading models like Rayleigh or Ricean [8].

Spatial modulation (SM) has been regard as as an energy-efficient method for multiple-input multiple-output (MIMO) systems in recent years [9]. This is due to the fact that only one antenna is active during transmission. In SM, the input bits are divided into two groups, one of which is modulated using amplitude/phase modulation (APM), such as M-ary modulation. The indices of the active antenna are used to map the other group of bits [10].

Index modulation orthogonal frequency division multiplexing (IM-OFDM), inspired by SM, has been proposed as a multicarrier technique for the frequency selective fading channel. In this technique, a part of the information bits is conveyed by the indices of the activated subcarriers [11], [12]. On the other hand, the other part of the information bits is conveyed by M-ary signal constellations similar to classical OFDM. This scheme archives a better bit error rate (BER) than the classical OFDM due to a higher degree of diversity realized by the index domain bits transmitted through a frequency selective fading channel [13]. Various schemes of IM techniques are surveyed in [12], [14], [15].

Previously, IM-OFDM has been investigated as a multiple-access technique for the uplink channel [16]–[20]. The rate of the IM-OFDM has been studied in [21], and a low detection method was proposed in [22]. Based on IM, a novel pilot design technique was provided for THz communication systems in [23], and a dual-mode technique for IM-OFDM was considered in [24]. A two-user cooperative scheme has been suggested in [25], [26]. Recently, IM-OFDM has been suggested as a multiple-access scheme for a downlink multiuser channel [27] in order to increase both the spectral efficiency (SE) and energy efficiency (EE) of the system. This is mainly because more information bits can be conveyed by the indices, where a limited number of subcarriers are activated during transmission leading to a reduction in the peak to average power ratio (PAPR). Also, it can avoid inter-user interference since each user is assigned a specific block of subcarriers. In index modulation multiple access (IMMA), as we consider in the first part of this paper, the OFDM subcarriers are divided into various sets, and each set is assigned to a specific user where its bits are transmitted via index modulation technique.

Moreover, in the second part, we propose an extended IMMA as a NOMA technique inspired by [28]. In this scheme, the transmitter partitions the users into different pairs, and each pair shares a block of OFDM subcarriers. The two users of each pair are allocated into different domains: the index domain and the constellation domain. The main advantages of this scheme are:

- It can double the number of users served at the same subcarrier block.
- While some papers have considered the combinations of both NOMA and IM [29], [30], the task of the detection

at the receiver was performed using SIC. In this scheme, we avoid the usage of such a complex receiver.
- In addition, the previous IM - NOMA schemes in [29], [30] tend to multiplex users over different levels of transmitted power. This causes interference between the users and hence affects the system performance. The proposed technique completely avoids such interference between the pairs, thus improving the system performance.

The main contributions of this paper can be summarized as follows:

- IMMA is considered a downlink multiple-access technique for the millimeter waves outdoor channel, and the error performance is analyzed.
- Another novel downlink multiple-access technique called extended IMMA is proposed based on the principle of spatial multiple access.
- Simulation results validate the superior ABER performance of both schemes over classical OFDMA and IM-NOMA, respectively.

The remainder of this paper is arranged in the following manner. The IMMA system model is illustrated in Section II. In Section III, the extended IMMA system model is presented. Section IV discusses the IMMA system's performance. In Section V, the simulation results are presented and discussed, and in Section VI, the paper is concluded.

II. SYSTEM MODEL OF IMMA
A. TRANSMITTER

Let us first consider the transmitter of downlink IMMA system as illustrated in Fig. 1. It consists of a single base station serving G users. Each user is assigned a subblock of OFDM subcarriers with length n, where $n = N/G$ and N is the number of total OFDM subcarriers, i.e., the size of the fast Fourier transform (FFT). For each user, only q out of n subcarriers are activated during transmission. A total number of P bits for each user enter the IMMA transmitter. Firstly, these bits are split into two groups: The first P_1 bits are responsible for the selection of the active subcarrier indices. Their function is to select which subcarrier index to be active during the transmission, and their size is calculated as

$$P_1 = \left\lfloor \log_2 \binom{n}{q} \right\rfloor. \tag{1}$$

The mapping process depends on a lookup table which is explained in Section II-B.

The remaining P_2 bits are modulated by M-ary modulation and then transmitted via the activated OFDM indices, and their size is calculated as

$$P_2 = q \log_2 M. \tag{2}$$

The total number of bits transmitted for each user can be written as

$$P = P1 + P2$$

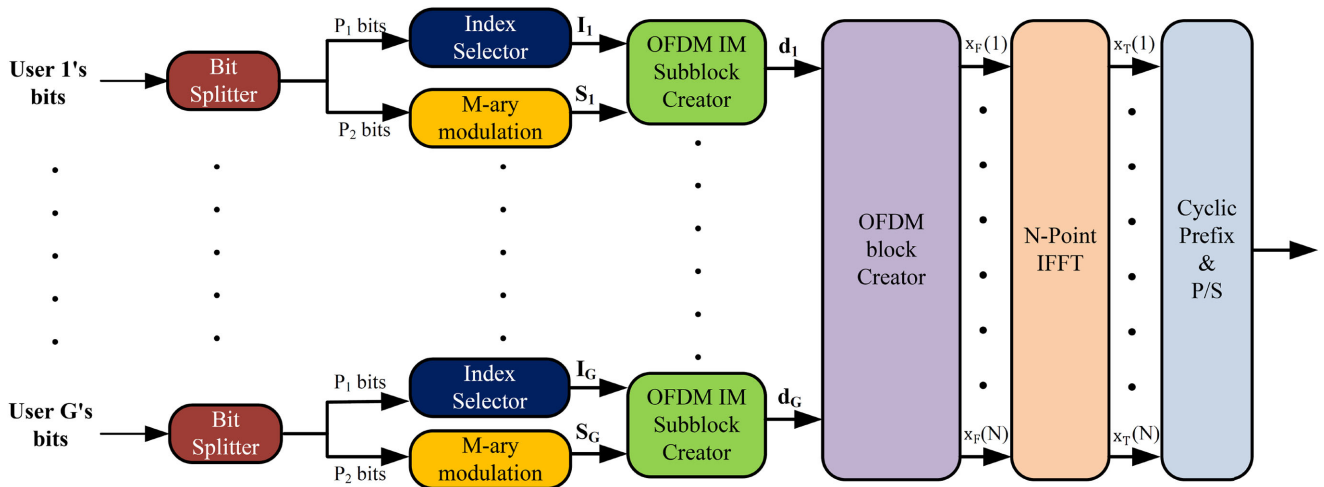$$= \lfloor \log_2 \binom{n}{q} \rfloor + q \log_2 M. \tag{3}$$

FIG. 1. IMMA transmitter block diagram.

The subblock output $\mathbf{d_g}$ of each user g; $1 \leq g \leq G$; can be written as

$$\mathbf{d_g} = \left[\underbrace{S_1\ 0\ \cdots\ 0\ S_2\ \cdots\ S_q\ 0}_{q\ \text{out of}\ n\ \text{non-zero values}} \right], \quad (4)$$

where S_q is the M-ary modulated symbols of P_2 bits. The location of the active q indices depends on the lookup table of P_1 bits. The vector $\mathbf{I_g}$ indicates the locations of active indices according to the lookup table. It can be represented as

$$\mathbf{I_g} = \left[\underbrace{1\ 0\ \cdots\ 0\ 1\ \cdots\ 1\ 0}_{q\ \text{out of}\ n\ \text{non-zero values}} \right]. \quad (5)$$

Next, the OFDM block creator concatenates all users' subblocks to create a single vector which has the dimension of $N \times 1$, which can be written as

$$\mathbf{x_F} = \begin{bmatrix} \mathbf{d_1} & \dots & \mathbf{d_g} \end{bmatrix}^T. \quad (6)$$

Similar to classical OFDM, the OFDM block is processed by the inverse Fast Fourier Transform (IFFT) algorithm:

$$\mathbf{x_T} = \frac{N}{\sqrt{q \times G}} \text{IFFT}\{\mathbf{x_F}\}. \quad (7)$$

After that, a cyclic prefix is then added to the block. The length of the cyclic prefix L must be greater than the channel impulse response v.

The spectral efficiency η for each user in the IMMA system can be written as

$$\eta = \frac{\lfloor \log_2 \binom{n}{q} \rfloor + q \log_2 M}{n}. \quad (8)$$

B. SUBCARRIER MAPPING

A look-up table is created at both the transmitter and receiver to identify the corresponding indices for the upcoming P_1 bits for each user and performs the opposite function at the user's

TABLE I Look up Table Example for $n = 4$ and $q = 2$

P_1 Bits	Activated Indices	Subblock's Output
[0 0]	1, 2	$[S_1 \quad S_2 \quad 0 \quad 0]$
[0 1]	2, 3	$[0 \quad S_1 \quad S_2 \quad 0]$
[1 0]	3, 4	$[0 \quad 0 \quad S_1 \quad S_2]$
[1 1]	1, 4	$[S_1 \quad 0 \quad 0 \quad S_2]$

receiver. Table I shows an example of a look-up table for $n = 4$ and $q = 2$.

C. SUBCARRIER ASSIGNMENT

There are basically two methods for subcarrier assignments: localized assignment or distributed one [31]. In the localized assignment, contiguous subcarriers are assigned to each user. On the other hand, subcarriers are assigned in a distributed manner to each user in the distributed technique. Fig. 2 illustrates the difference between the two methods.

D. 28 GHZ CHANNEL MODEL

The fluctuating two-ray (FTR) fading model is the multipath fading channel model for 28 GHz [8]. Two fluctuating components, as well as random phase and diffuse components, make up this channel model. It evolved from the two-wave with diffuse power (TWDP) fading model introduced in [32]. The FTR fading distribution fits the 28 GHz field measurements results in [8] considerably better than Rician fading. The complex baseband received signal in the FTR model can be expressed as

$$V_r = \sqrt{\zeta}V_1\exp(j\phi_1) + \sqrt{\zeta}V_2\exp(j\phi_2) + X + jY, \quad (9)$$

where $V_n\exp(j\phi_n)$ is the nth component with uniformly distributed phase ϕ_n and a constant amplitude V_n. The diffuse received signal component is represented by $X + jY$, a complex Gaussian random variable with a distribution $\mathbb{N}(0, \sigma^2)$.
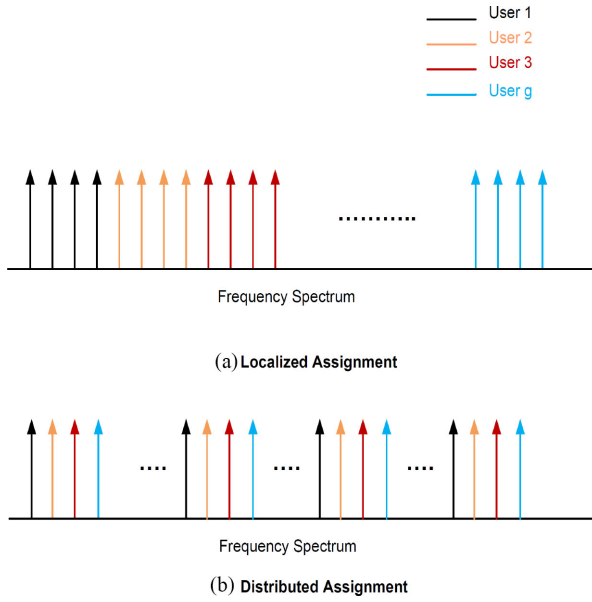
(a) **Localized Assignment**

(b) **Distributed Assignment**

FIG. 2. Localized vs. Distributed Assignment.

TABLE II The Relation Between FTR Model Parameters and Classical Fading Channels

Fading Channel	FTR model parameters (Δ, K, m)
Rayleigh	$\Delta = 0, K \to \infty, m = 1$
Ricean-(K)	$\Delta = 0, K = K, m \to \infty$
Nakagami-(m)	$\Delta = 0, K \to \infty, m = m$

The three parameters that characterize the FTR model are as follows:

$$K = \frac{V_1{}^2 + V_2{}^2}{2\sigma^2}, \qquad (10)$$

$$\Delta = \frac{2V_1 V_2}{V_1{}^2 + V_2{}^2}, \qquad (11)$$

ζ is a Gamma distributed random variable and has the following PDF.

$$f_\zeta(x) = \frac{m^m x^{(m-1)}}{\Gamma(m)} e^{(-mx^2)}. \qquad (12)$$

The ratio of the average power of the dominating components to the power of the remaining diffuse multipath is denoted by K. The similarity between the received powers from the dominating components is represented by Δ. The relation between the FTR model and classical fading channel models (Rayleigh, Rician, and Nakagami-m) [8] is summarised in Table II.

E. IMMA RECEIVER

After the transmitter, the signal is transmitted through a frequency-selective fading channel between the transmitter and user g. The channel can be represented by the following channel impulse response (CIR) coefficients with
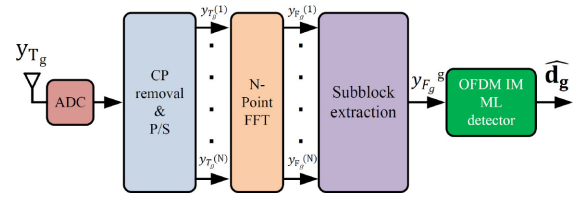
FIG. 3. Block diagram of IMMA receiver.

delay taps v.

$$\mathbf{h_{T_g}} = \left[h_{T_g}(1) \ h_{T_g}(2) \ \cdots \ h_{T_g}(v) \right]^T. \qquad (13)$$

After passing through the channel, the received signal at each user in the frequency domain after removing the cyclic prefix can be written as

$$y_{F_g}(\alpha) = x_F(\alpha) h_{F_g}(\alpha) + w_{F_g}(\alpha), \quad 1 \le \alpha \le N, \qquad (14)$$

where y_{F_g}, h_{F_g}, and w_{F_g} are the received signals, the channel fading coefficients and the noise samples in the frequency domain at user g respectively. w_{F_g} has a distribution $\mathcal{CN}(0, N_F)$.

The structure of each user's receiver is shown in Fig. 3. Its tasks are first to remove the cyclic prefix and perform N-point FFT. After that, it needs to extract its own subcarriers data, which can be symbolized as $y_{F_g}{}^g$ with the corresponding subcarriers fading channel coefficients $h_{F_g}{}^g$ in the frequency domain. Thus, the received signal after subcarrier extraction for each user can be written as

$$y_{F_g}{}^g(\beta) = d_g(\beta) h_{F_g}{}^g(\beta) + w_{F_g}{}^g(\beta), \quad 1 \le \beta \le n. \qquad (15)$$

The maximum likelihood (ML) detector considers all possible IM-subblock realizations by searching for all the possible combinations between the subcarrier indices and the signal constellation points in order to make a joint decision to estimate both the transmitted constellation symbols $\widehat{S}_g$ and the active indices $\widehat{I}_g$ by minimizing the following metric

$$[\widehat{I}_g, \widehat{S}_g] = \arg\min_{I_g, S_g} \sum_{\beta=1}^{n} \left| y_{F_g}{}^g(\beta) - h_{F_g}{}^g(\beta) d_g(\beta) \right|^2. \qquad (16)$$

After estimating $\widehat{S}_G$, it will be M-ary demodulated to get $\widehat{P}_2$ bits. The lookup table at the receiver will convert $\widehat{I}_G$ to the estimated $\widehat{P}_1$ bits.

III. SYSTEM MODEL OF EXTENDED IMMA
A. TRANSMITTER

In this scheme, we consider serving multiple pairs U of users. Each pair is allocated a specific set of OFDM subcarriers, and it consists of two users: the IM user and the APM one. The bits of the IM user are responsible for the activation of the subcarrier indices. This process can be done through the lookup table as in IMMA. On the other hand, the bits of the APM user are modulated by M-ary modulation then transmitted via the activated OFDM indices assigned to its own pair.
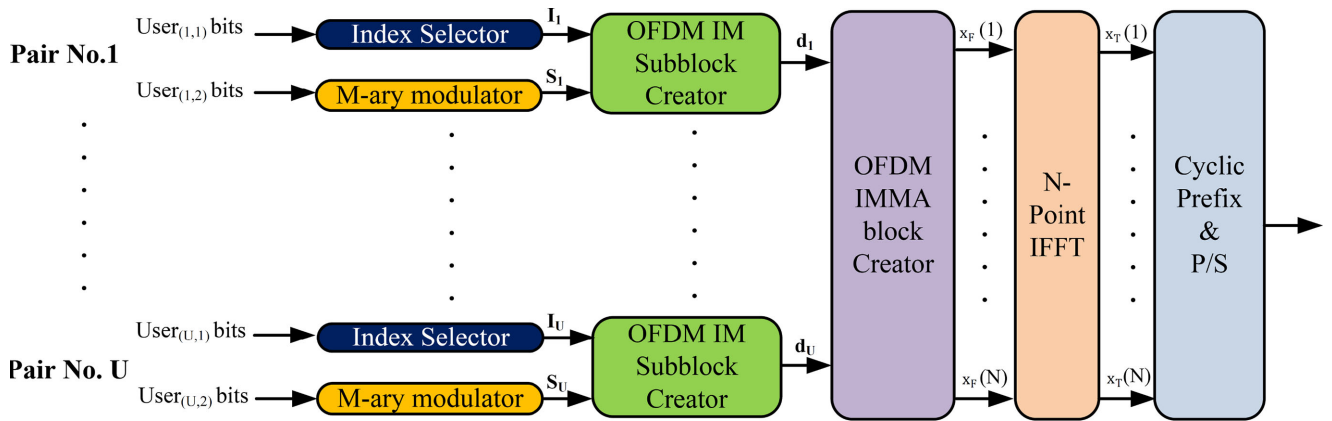
FIG. 4. Extended IMMA transmitter block diagram.

The transmitter block diagram is as shown in Fig. 4. This diagram consists of U pairs of users. The 1st user in each pair is the IM user whose bits are processed by the index selector to determine which indices to be active according to the lookup table. The 2nd user in each pair is the APM one whose bits are mapped by the M-ary modulator.

For each pair, The OFDM IM subblock creator emits the M-ary constellation symbols through the activated indices to produce the output vector D_u similar to (4). After that, the OFDM block creator concatenates all the outputs from different pairs to form $N \times 1$ OFDM block processed by N-point IFFT. After that, A cyclic prefix is added, and the output block is treated as classical OFDMA.

If each pair is assigned z subcarriers, the spectral efficiency for the IM user and APM one; η_i and η_p respectively; in the extended IMMA system can be written as

$$\eta_i = \frac{\lfloor \log_2 \binom{z}{q} \rfloor}{z}. \tag{17}$$

$$\eta_p = \frac{q \log_2 M}{z}. \tag{18}$$

After passing through the channel, the received signal in the case of extended IMMA can be written as

$$y_{F_{u,i}}(\alpha) = x_F(\alpha) h_{F_{u,i}}(\alpha) + n_{F_{u,i}}(\alpha), \quad 1 \le \alpha \le N, \tag{19}$$

where $y_{F_{u,i}}$, $h_{F_{u,i}}$ and $n_{F_{u,i}}$ are the received signals, the channel fading coefficients, and the noise samples in the frequency domain at user $i; i \in [1, 2]$; in the uth pair.

B. IM USER'S RECEIVER

The structure of the receiver is similar to the IMMA receiver in Fig. 3. For this user's receiver, its task is to extract its own bits via detecting the indices of the active subcarriers. In order to do that, the user's receiver has to extract the received data allocated on its pair's subcarriers, which can be symbolized as $y_{F_{u,1}}{}^u$ with the corresponding subcarriers fading channel coefficients $h_{F_{u,1}}{}^u$ in the frequency domain. Thus, the received signal after subcarrier extraction for the IM user can be

written as

$$y_{F_{u,1}}{}^u(\gamma) = d_u(\gamma) h_{F_{u,1}}{}^u(\gamma) + n_{F_{u,1}}^u(\gamma), \quad 1 \le \gamma \le z. \tag{20}$$

The ML detector considers all possible subblock realizations by searching for all possible subcarrier index combinations and the signal constellation points in order to make a decision to determine the active indices only.

$$\widehat{I_u} = \arg \min_{I_u, S_u} \sum_{\gamma=1}^{z} \left| y_{F_{u,1}}{}^u(\gamma) - h_{F_{u,1}}{}^u(\gamma) d_u(\gamma) \right|^2. \tag{21}$$

C. APM USER'S RECEIVER

The structure of the receiver is similar to the IMMA receiver in Fig. 3. After the N-point FFT, the receiver extracts its corresponding subcarriers. Then it performs a maximum ratio combining (MRC) based detection, which consists of two steps inspired by [33]. In the two-step method, the indices of the activated indices are firstly decoded. Then, the M-ary symbols on the activated resources are further decoded to get the information bits for this user.

IV. PERFORMANCE ANALYSIS OF IMMA

The average BER can be expressed through the well-known union bounding technique as

$$ABER \le \frac{1}{P \times 2^P} \sum_{\mathbf{d_g}} \sum_{\widehat{\mathbf{d_g}} \ne \mathbf{d_g}} N(\mathbf{d_g}, \widehat{\mathbf{d_g}}) \times P_e(\mathbf{d_g} \to \widehat{\mathbf{d_g}}), \tag{22}$$

where $N(\mathbf{d_g}, \widehat{\mathbf{d_g}})$ is the hamming distance between $\mathbf{d_g}$ and $\widehat{\mathbf{d_g}}$. $P_e(\mathbf{d_g} \to \widehat{\mathbf{d_g}})$ represents the pairwise error probability (PEP) if $\widehat{\mathbf{d_g}}$ is detected given that $\mathbf{d_g}$ is transmitted. Using matrix notation, (15) can be re-written as

$$\mathbf{y} = \mathbf{H}\mathbf{d_g} + \mathbf{w}, \tag{23}$$

where $\mathbf{y} = [y_{F_g}{}^g(1) \cdots y_{F_g}{}^g(n)]^T$, $\mathbf{H}$ is an $n \times n$ all-zero matrix except for its main diagonal elements denoted by $h_{F_g}{}^g(1) \cdots h_{F_g}{}^g(n)$. Let us define $\mathbf{w} = [w_{F_g}{}^g(1) \cdots w_{F_g}{}^g(n)]^T$.

Eq(16) can be re-written as

$$\widehat{\mathbf{d_g}} = \arg \min_{\mathbf{d_g}} \|\mathbf{y} - \mathbf{H}\mathbf{d_g}\|_F^2. \tag{24}$$

The conditional PEP on $\mathbf{H}$ can be expressed with the aid of the Q-function as

$$P_e\left(\mathbf{d_g} \to \widehat{\mathbf{d_g}}\right) = Q\left(\sqrt{\frac{\xi}{2 \times N_F}}\right), \tag{25}$$

where $\xi = \|\mathbf{H}\Psi\|_F^2$ and $\Psi = (\mathbf{d_g} - \widehat{\mathbf{d_g}})$. Thus $\xi = \sum_{\lambda=1}^{n} \|h(\lambda)\Psi(\lambda)\|_F^2$. The PDF of $\Lambda = \|h(\lambda)\|_F^2$ can be expressed as

$$f_\Lambda(\Lambda) = \frac{1}{2r} f_r(r^2), \tag{26}$$

where $f_r(r)$ is given in [8, (15)] with r^2 replaced by Λ. The moment generating function (MGF) [34] is expressed as

$$M_\Lambda(s) = \int_0^\infty f_\Lambda(\Lambda) e^{s\Lambda} d\Lambda. \tag{27}$$

Since only q out of n subcarriers are active during transmission, the MGF of ξ can be expressed as follows

$$M_\xi(s) = \prod_{i=1}^{q} M_{\Lambda_i}(s),$$
$$= (M_\Lambda(s))^q. \tag{28}$$

Using the previous MGF, the PDF of ξ can be written as

$$f_\xi(\xi) = \frac{1}{2\pi} \int_{-\infty}^{\infty} \left(\int_0^\infty f_\Lambda(\Lambda) e^{s\Lambda} d\Lambda\right)^q e^{-s\Lambda} ds. \tag{29}$$

Now, the unconditional PEP can be computed by integrating (25) over $f_\xi(\xi)$ as

$$P_e\left(\mathbf{d_g} \to \widehat{\mathbf{d_g}}\right) = \int_0^\infty Q\left(\sqrt{\frac{\xi}{2 \times N_F}}\right) f_\xi(\xi) d\xi. \tag{30}$$

V. NUMERAL RESULTS

For the upcoming results, the FTR millimeter waves channel is used as the fading channel with 10 delay taps. The number of OFDM subcarriers is $N = 128$, with a cyclic prefix is 16. Matlab is used for the simulation with 10^7 channel realization.

In Fig. 5., we compare the performance of both OFDMA and IMMA in the Rayleigh channel scenario and FTR channel model with the following parameters $\Delta = 0, K = 100(\to \infty)$, and $m = 1$. In OFDMA, each user is assigned 4 subcarriers with BPSK as the modulation scheme. For IMMA, each user is assigned $n = 4$ subcarriers with $q = 2$ and, BPSK is used as the modulation scheme. The performance of the OFDMA system is precisely the same in both Rayleigh and FTR channels, which validates the approximation in table II. This fact also exists for the IMMA system performance. At a BER value of 10^{-5}, the IMMA achieves approximately 7 dB better BER performance than the OFDMA. This is due to the higher diversity archived by the bits transmitted via the active indices.
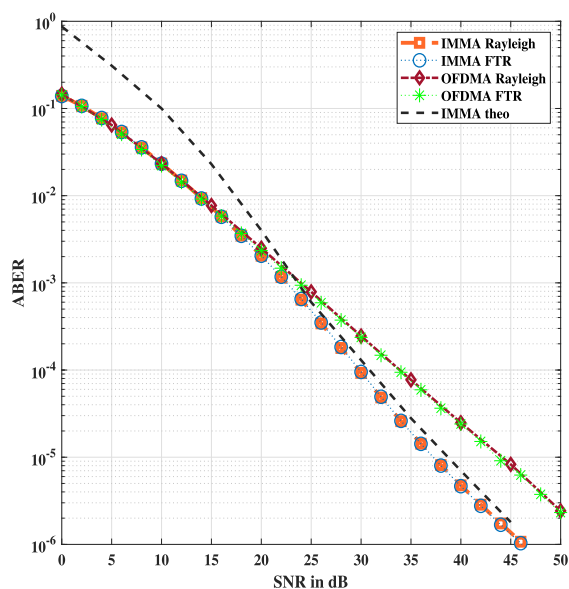

FIG. 5. ABER performance of OFDMA and IMMA in Rayleigh channel and FTR approximation $\Delta = 0, K = 100(\to \infty), m = 1$.
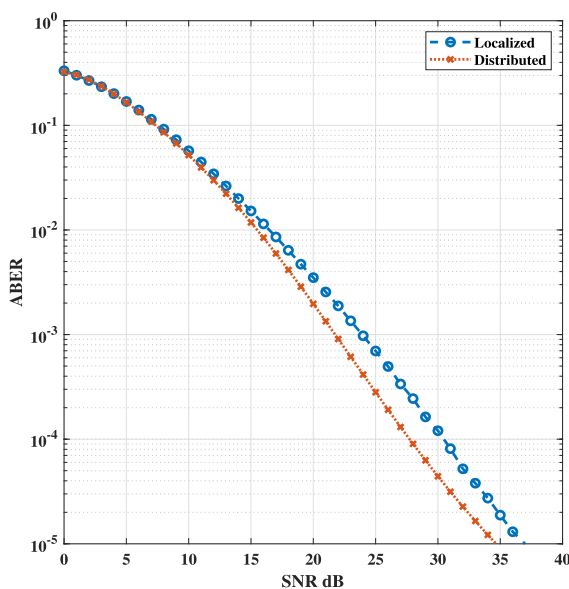

FIG. 6. ABER performance of IMMA for different techniques of subcarrier assignment.

Fig. 6. shows the BER performance for different techniques of subcarrier resource assignment in the IMMA system in the millimeter waves channel with parameters ($\Delta = 0.2, K = 10, m = 2$). In this simulation, 4 users are being served so that each user is allocated only 32 subcarriers ($n = 32, q = 1$) and using 4-QAM as the modulation scheme. It is clear that the distributed technique has a slightly better performance than the localized one. This is mainly because the distributed one provides a higher degree of diversity over the channel response, which leads to an improvement in BER evaluation.

Fig. 7. shows the average BER performance of the 32 users for different modulation order M vs. SNR in millimeter
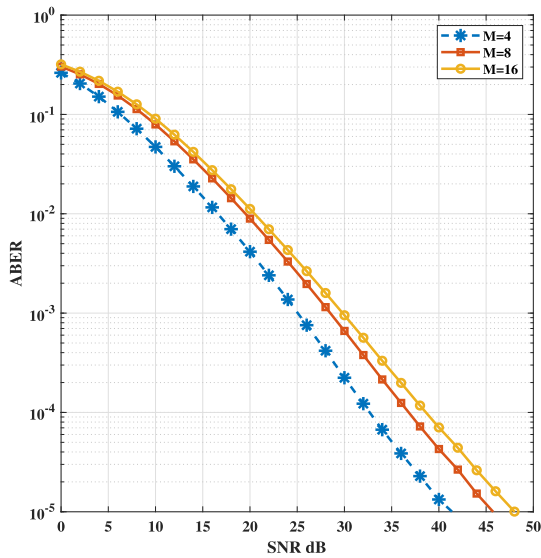
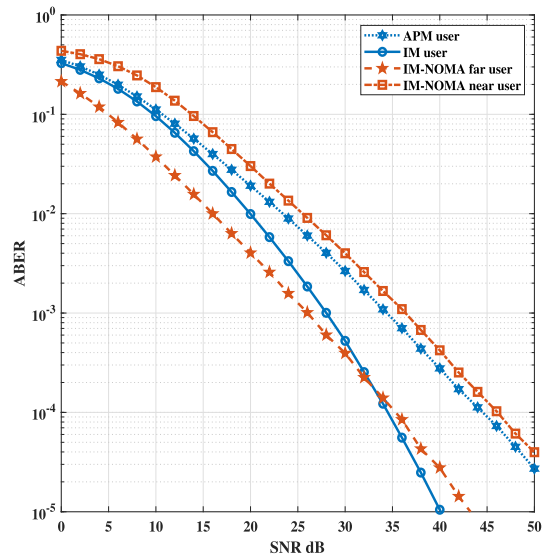**FIG. 7.** ABER performance of IMMA for different modulation order *M*.

FIG. 9. ABER performance of extended IMMA and IM-NOMA.
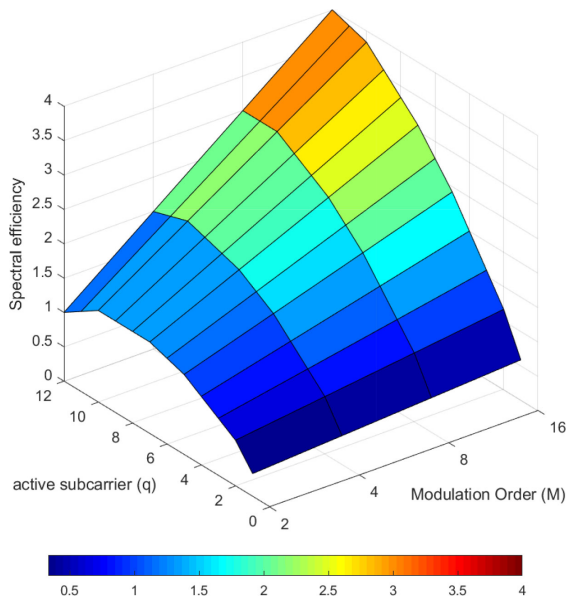

FIG. 8. Spectral efficiency of IMMA system.

waves channel with parameters ($\Delta = 0.3, K = 8, m = 3$). In this simulation, 32 users are being served so that each user is allocated only 4 subcarriers ($n = 4, q = 2$) and using QAM as the modulation scheme. It is clear that as the modulation order increases, the ABER performance gets worsen due to increasing the number of bits transmitted by each symbol of the IMMA system.

Fig. 8. illustrates how the spectral efficiency per user of the IMMA system changes as a function of the number of active subcarriers q and modulation order M where $n = 12$. We can notice that: As M increases, the SE also increases linearly. However, a non-linear increase is archived as q increases.

The ABER performance of the extended IMMA is studied in Fig. 9. in the millimeter waves channel with parameters

($\Delta = 0.1, K = 10, m = 5$). In order to make a fair comparison between the performance of the APM user and the IM one, the modulation order $M = 4$ is chosen to be equal to z with $q = 1$. The IM user has archived a better ABER performance than the APM one. This is mainly because transmission via the IM is affected by a higher diversity of different subcarriers. This concept was argued in [35], where space shift keying was compared to the classical M-ary modulation. The extended IMMA has archived an improved ABER performance than the IM-NOMA presented in [29]. In order to make a fair comparison, IM-NOMA parameters were selected to be the same as the ones used for extended IMMA, i.e., number of total subcarriers and cyclic prefix. The power allocation factor is chosen to be 0.25.

VI. CONCLUSION
In this paper, index modulation multiple access is presented as a multiple access technique for millimeter waves outdoor channel. In our study, different subcarrier mapping techniques are considered. The results reveal that IMMA archives better performance in comparison with the classical OFDMA. Moreover, extended IMMA is proposed as a NOMA system to avoid the drawbacks of IM-NOMA techniques such as inter-user interference and usage of complex receivers such as successive interference cancellation (SIC). Both techniques are shown to be energy efficient since limited numbers of subcarriers are active during transmission. The superior performance compared with the previous IM-based NOMA scheme is validated through numerical simulations.

REFERENCES
[1] M. Agiwal, A. Roy, and N. Saxena, "Next generation 5G wireless networks: A comprehensive survey," *IEEE Commun. Surv. Tut.*, vol. 18, no. 3, pp. 1617–1655, Jul.–Sep. 2016.
[2] J. G. Andrews *et al.*, "What will 5G be?" *IEEE J. Sel. Areas Commun.*, vol. 32, no. 6, pp. 1065–1082, Jun. 2014.

[3] L. Dai, B. Wang, Y. Yuan, S. Han, I. Chih-Lin, and Z. Wang, "Non-orthogonal multiple access for 5G: Solutions, challenges, opportunities, and future research trends," *IEEE Commun. Mag.*, vol. 53, no. 9, pp. 74–81, Sep. 2015.

[4] Y. Saito, Y. Kishiyama, A. Benjebbour, T. Nakamura, A. Li, and K. Higuchi, "Non-orthogonal multiple access (NOMA) for cellular future radio access," in *Proc. IEEE 77th Veh. Technol. Conf.*, 2013, pp. 1–5.

[5] R. Hoshyar, F. P. Wathan, and R. Tafazolli, "Novel low-density signature for synchronous CDMA systems over AWGN channel," *IEEE Trans. Signal Process.*, vol. 56, no. 4, pp. 1616–1626, Apr. 2008.

[6] H. Nikopour and H. Baligh, "Sparse code multiple access," in *Proc. IEEE 24th Annu. Int. Symp. Pers., Indoor, Mobile Radio Commun.*, 2013, pp. 332–336.

[7] Z. Pi and F. Khan, "An introduction to millimeter-wave mobile broadband systems," *IEEE Commun. Mag.*, vol. 49, no. 6, pp. 101–107, Jun. 2011.

[8] J. M. Romero-Jerez, F. J. Lopez-Martinez, J. F. Paris, and A. J. Goldsmith, "The fluctuating two-ray fading model: Statistical characterization and performance analysis," *IEEE Trans. Wireless Commun.*, vol. 16, no. 7, pp. 4420–4432, Jul. 2017.

[9] R. Y. Mesleh, H. Haas, S. Sinanovic, C. W. Ahn, and S. Yun, "Spatial modulation," *IEEE Trans. Veh. Technol.*, vol. 57, no. 4, pp. 2228–2241, Jul. 2008.

[10] M. D. Renzo, H. Haas, A. Ghrayeb, S. Sugiura, and L. Hanzo, "Spatial modulation for generalized MIMO: Challenges, opportunities, and implementation," *Proc. IEEE*, vol. 102, no. 1, pp. 56–103, Jan. 2014.

[11] E. Başar, Ü. Aygölü, E. Panayırcı, and H. V. Poor, "Orthogonal frequency division multiplexing with index modulation," *IEEE Trans. Signal Process.*, vol. 61, no. 22, pp. 5536–5549, Nov. 2013.

[12] T. Mao, Q. Wang, Z. Wang, and S. Chen, "Novel index modulation techniques: A survey," *IEEE Commun. Surv. Tut.*, vol. 21, no. 1, pp. 315–348, Jan.–Mar. 2019.

[13] E. Basar, "Index modulation techniques for 5G wireless networks," *IEEE Commun. Mag.*, vol. 54, no. 7, pp. 168–175, Jul. 2016.

[14] S. D. Tusha, A. Tusha, E. Basar, and H. Arslan, "Multidimensional index modulation for 5G and beyond wireless networks," *Proc. IEEE*, vol. 109, no. 2, pp. 170–199, Feb. 2021.

[15] E. Basar, M. Wen, R. Mesleh, M. Di Renzo, Y. Xiao, and H. Haas, "Index modulation techniques for next-generation wireless networks," *IEEE Access*, vol. 5, pp. 16693–16746, 2017, doi: 10.1109/ACCESS.2017.2737528.

[16] S. Althunibat, R. Mesleh, and T. F. Rahman, "A novel uplink multiple access technique based on index-modulation concept," *IEEE Trans. Commun.*, vol. 67, no. 7, pp. 4848–4855, Jul. 2019.

[17] M. B. Shahab, S. J. Johnson, M. Shirvanimoghaddam, M. Chafii, E. Basar, and M. Dohler, "Index modulation aided uplink NOMA for massive machine type communications," *IEEE Wireless Commun. Lett.*, vol. 9, no. 12, pp. 2159–2162, Dec. 2020.

[18] Y.-T. Lai, Y.-R. Ciou, and J.-M. Wu, "Index modulation multiple access," in *Proc. IEEE 29th Annu. Int. Symp. Pers., Indoor Mobile Radio Commun.*, 2018, pp. 1–5.

[19] W. Belaoura, S. Althunibat, K. Qaraqe, and K. Ghanem, "Precoded index modulation based multiple access scheme," *IEEE Trans. Veh. Technol.*, vol. 69, no. 11, pp. 12912–12920, Nov. 2020.

[20] S. Althunibat, R. Mesleh, and K. A. Qaraqe, "IM-OFDMA: A novel spectral efficient uplink multiple access based on index modulation," *IEEE Trans. Veh. Technol.*, vol. 68, no. 10, pp. 10315–10319, Oct. 2019.

[21] M. Wen, X. Cheng, M. Ma, B. Jiao, and H. V. Poor, "On the achievable rate of OFDM with index modulation," *IEEE Trans. Signal Process.*, vol. 64, no. 8, pp. 1919–1932, Apr. 2016.

[22] J. Li, Q. Li, S. Dang, M. Wen, X.-Q. Jiang, and Y. Peng, "Low-complexity detection for index modulation multiple access," *IEEE Wireless Commun. Lett.*, vol. 9, no. 7, pp. 943–947, Jul. 2020.

[23] T. Mao and Z. Wang, "Terahertz wireless communications with flexible index modulation aided pilot design," *IEEE J. Sel. Areas Commun.*, vol. 39, no. 6, pp. 1651–1662, Jun. 2021.

[24] T. Mao, Z. Wang, Q. Wang, S. Chen, and L. Hanzo, "Dual-mode index modulation aided OFDM," *IEEE Access*, vol. 5, pp. 50–60, 2017, doi: 10.1109/ACCESS.2016.2601648.

[25] X. Chen, M. Wen, and S. Dang, "On the performance of cooperative OFDM-NOMA system with index modulation," *IEEE Wireless Commun. Lett.*, vol. 9, no. 9, pp. 1346–1350, Sep. 2020.

[26] X. Chen, M. Wen, T. Mao, and S. Dang, "Spectrum resource allocation based on cooperative NOMA with index modulation," *IEEE Trans. Cogn. Commun. Netw.*, vol. 6, no. 3, pp. 946–958, Sep. 2020.

[27] Q. Li, M. Wen, B. Clerckx, S. Mumtaz, A. Al-Dulaimi, and R. Q. Hu, "Subcarrier index modulation for future wireless networks: Principles, applications, and challenges," *IEEE Wireless Commun.*, vol. 27, no. 3, pp. 118–125, Jun. 2020.

[28] C. Zhong, X. Hu, X. Chen, D. W. K. Ng, and Z. Zhang, "Spatial modulation assisted multi-antenna non-orthogonal multiple access," *IEEE Wireless Commun.*, vol. 25, no. 2, pp. 61–67, Apr. 2018.

[29] E. Arslan, A. T. Dogukan, and E. Basar, "Index modulation-based flexible non-orthogonal multiple access," *IEEE Wireless Commun. Lett.*, vol. 9, no. 11, pp. 1942–1946, Nov. 2020.

[30] A. Almohamad, M. O. Hasna, S. Althunibat, and K. Qaraqe, "A novel downlink IM-NOMA scheme," *IEEE Open J. Commun. Soc.*, vol. 2, pp. 235–244, 2021. [Online]. Available: https://ieeexplore.ieee.org/document/9324769

[31] S. Ahmadi, *5G NR: Architecture, Technology, Implementation, and Operation of 3GPP New Radio Standards*. New York, NY, USA: Academic, 2019, pp. 315–330.

[32] G. D. Durgin, T. S. Rappaport, and D. A. D. Wolf, "New analytical models and probability density functions for fading in wireless communications," *IEEE Trans. Commun.*, vol. 50, no. 6, pp. 1005–1015, Jun. 2002.

[33] M. Maleki, H. R. Bahrami, and A. Alizadeh, "On MRC-based detection of spatial modulation," *IEEE Trans. Wireless Commun.*, vol. 15, no. 4, pp. 3019–3029, Apr. 2016.

[34] M. K. Simon and M.-S. Alouini, *Digital Communication Over Fading Channels*, vol. 95. Hoboken, NJ, USA: Wiley, 2005, pp. 4–5.

[35] J. Jeganathan, A. Ghrayeb, L. Szczecinski, and A. Ceron, "Space shift keying modulation for MIMO channels," *IEEE Trans. Wireless Commun.*, vol. 8, no. 7, pp. 3692–3703, Jul. 2009.

SAID E. EL-KHAMY (Life Fellow, IEEE) received the B.Sc. (Hons.) and M.Sc. degrees from Alexandria University, Alexandria, Egypt, in 1965 and 1967, respectively, and the Ph.D. degree from the University of Massachusetts, Amherst, MA, USA, in 1971. He has been a Teaching Staff with the Department of Electrical Engineering, Faculty of Engineering, Alexandria University, Alexandria, Egypt, since 1972, and was appointed as a Fulltime Professor in 1982 and as the Chairman of the Electrical Engineering Department from September 2000 to September 2003 and is currently an Emeritus Professor.

He has authored or co-authored about four hundred scientific papers in national and international conferences and journals. His current research interests include wireless multimedia communications, wave propagation, smart antenna arrays, modern signal processing techniques, image processing, and security and watermarking techniques. He took part in the organization of many local and international conferences including the yearly series of NRSC (URSI) conference series from 1990 to 2019, ISCC'95, ISCC'97, ISSPIT'2000, MELECON'2002, and IEEE GCIoT'2019. He took part in many IEEE Region 8 activities as well as URSI general assemblies.

Prof. El-Khamy has earned many national and international research Awards among which are the R.W.P. King Best Paper Award of the Antennas and Propagation Society of IEEE in 1980, Egypt's State Engineering Encouraging Research Award for two times in 1980 and 1989, respectively, Abdel-Hamid Schoman-Kingdom of Jordan Award for Engineering Research in 1982, State Scientific Excellence Award in Engineering Sciences for 2002, Alexandria University Appreciation Award of Engineering Sciences for 2003, State Appreciation Award of Engineering Sciences for 2004 as well as the IEEE Region 8 Volunteer Award for 2010. In 2016, he was Honored by Egypt's National Radio Science Committee of URSI and was selected as the Radio Science recognized figure of the year. Also, in 2016, he was announced to be the "The Distinct Scientist of Alexandria University, in Engineering Sciences".

He is also a Fellow of the Electromagnetic Academy and URSI Senior Member. He is the Founder and past President of IEEE Alexandria/Egypt Subsection and the past President of Egypt's National Radio Science Committee of URSI.

HASSAN M. ELRAGAL received the B.Sc. and M.Sc. degrees in electrical engineering from Alexandria University, Alexandria, Egypt, in 1991 and 1995, respectively. In July 2001, he received the Ph.D. degree in electrical engineering from Southern Methodist University in Dallas, Texas TX, USA. His research interests include signal processing, fuzzy logic, neural networks, genetic algorithms, and particle swarm optimization.

REMON A. POLUS (Student Member, IEEE) received the B.Sc. and M.Sc. degrees in electrical engineering from Alexandria University, Alexandria, Egypt, in 2016 and 2021, respectively. He has been working as a Teaching Assistant with the Department of Electrical Engineering, Alexandria University since 2017. His current research interests include wireless communications, signal processing, and MIMO systems.